

# Non-destructive characterization of internal surfaces in Laser Powder Bed Fused Inconel 718 channels prior and after post-treatment

Galina Kasperovich<sup>1</sup>, Katia Artzt<sup>1</sup>, Guillermo Requena<sup>1,2</sup>, Ralf Becker<sup>3</sup>, Thomas Behrendt<sup>3</sup>, Jan Haubrich<sup>1</sup>

<sup>1</sup>Institute of Materials Research, German Aerospace Center (DLR), Linder Hoehe, D-51147 Cologne, Germany

<sup>2</sup>Metallic Structures and Materials Systems for Aerospace Engineering, RWTH University, D-52062 Aachen, Germany

<sup>3</sup>Institute of Propulsion Technology, German Aerospace Center (DLR), Linder Hoehe, D-51147 Cologne, Germany

[galina.kasperovich@dlr.de](mailto:galina.kasperovich@dlr.de), [katia.artzt@dlr.de](mailto:katia.artzt@dlr.de), [guillermo.requena@dlr.de](mailto:guillermo.requena@dlr.de), [ralf.becker@dlr.de](mailto:ralf.becker@dlr.de),

[thomas.behrendt@dlr.de](mailto:thomas.behrendt@dlr.de), [jan.haubrich@dlr.de](mailto:jan.haubrich@dlr.de)

## Abstract

The effect of surface finishing treatments for inner surfaces of additively manufactured Inconel 718 specimens were analyzed using X-ray computed tomography (CT). The tube-shaped specimens were built by Laser Powder Bed Fusion (LPBF) at different build orientations and the inner surface characteristics such as roundness, equivalent diameter, 3D curvature distribution and distance to nominal surface as radial roughness for internal channels, both in the primary “as built” condition and after the subsequent treatment, were evaluated.

Keywords: LPBF, Inconel 718, internal channels, surface treatment, computer tomography

## 1 Introduction

Additive manufacturing (AM) of metals, in particular Laser Powder Bed Fusion (LPBF), allows the production of geometrically complex components with integrated functional features such as precise internal cavities for fuel or cooling channels. In this context, Nickel-based superalloys such as Inconel 718 are of great interest for use in modern turbine engines.

In LPBF complex components can be manufactured with advanced cooling systems consisting of many multi-directional thin inner channels. Surface roughness and dimensional tolerance of internal channels are critical for the intended turbine engine applications. Cooling channels require a well-defined mass flow rate per given pressure drop in order to minimize uncertainties in the thermal design of combustor walls. In fuel lines and injectors, the surface roughness affects the propensity to fuel coking which deteriorates fuel distribution and may result in local blockage. The channel quality is determined by the LPBF process parameters and depends on the orientation during the production stage [1]. However, the complexity of the combustion chamber design, combined with multidirectional channels, does not allow complete prevention of defects of the downskin surfaces and may require a subsequent surface treatment. For this purpose, methods of chemical etching are used in particular. The use of X-ray computed tomography enabled non-destructive quantitative characterization of the surface quality and channel properties prior and after post-treatment.

## 2. Formation of curved inner surfaces using LPBF and quantitative analysis method

In LPBF the build direction of a component or specimen plays a decisive role for the obtainable surface qualities of inner channels (Figure 1(a)): the lower the build inclination with respect to the working platform (XY), the greater is the curvature of the channel geometry and the larger the area fraction corresponding to downskin surfaces. Thus, for example, when the orientation is decreased from 90° (vertical build orientation) to 0° (horizontal), the roundness of the shape is more than halved. A more detailed analysis of the build orientation effect and optimization measures to improve it are presented in [1]. The optimized volumetric and contouring parameters for Inconel 718 obtained in [1] are used for manufacturing the specimens in the present study.

Tube-shaped specimen with an inner diameter of 2 mm and a length of 200 mm were produced from Inconel 718 powder on a ConceptLaser M2 (200 W) machine (GE Additive company, Germany) at build inclinations of 0°, 30°, 60° and 90° (Figure 1 (a)). After the build process, the specimens were heat treated for stress relieving in accordance with standard AMS 5662, namely: kept at 720 °C for 8 hours, cooled in furnace to 620 °C, kept again at 620 °C for 8 hours and then cooled in air.

As a post-treatment of internal surfaces, an etching solution was used, which was passed through the channel with a given time, pressure and composition. The specific etching data are the know-how of the companies involved and are not given here. To present the methodology of internal channel analysis before and after treatment by means of non-destructive CT, two different surface finishing methods were chosen, hereinafter referred to as method 1 and method 2.

All samples were examined before and after post-treatment using a Phoenix Nanotom tomography (phoenix|x-ray Systems + Services GmbH, Germany) with a source voltage of 100 kV, a current of 120 mA, an exposure time of 2000 ms and an

averaging/skip of 3/1 with 360° rotation (Figure 1 (b)). The resulting pixel size was 2.3 μm. The raw data was converted from the software phoenix\_datos|x\_2\_aquisition via phoenix\_datos|x\_2\_reconstruction (Figure 1(c), GE Sensing & Inspection Technologies GmbH, Germany) into stacks of 1600 two-dimensional (2D) slices that were finally analysed as three-dimensional (3D) volumes in the software AVIZO (Thermo Fisher Scientific Inc.). The middle parts of all 200 mm long samples were examined both before and after treatment.

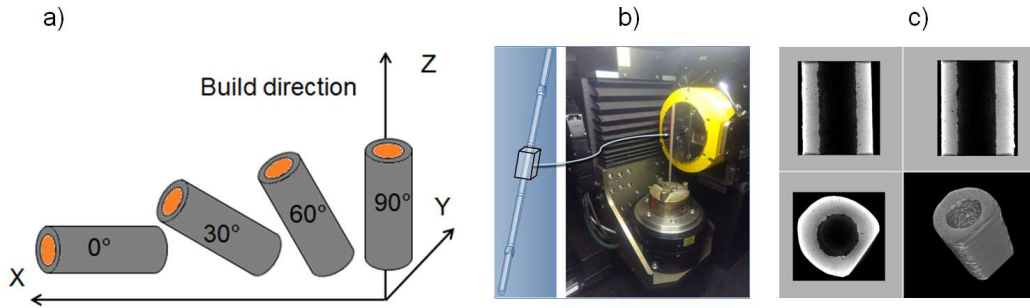


Figure 1: Build orientation of the samples with an inner diameter of 2 mm (orange inside) in relation to the working platform (a), tomographic examination of the middle part of the sample (b) and an example of primary reconstruction (c).

The reconstructed channels were evaluated quantitatively: the geometric deviation from the target shape was analysed in 2D on cross sections of the channels (in total 1600 slices per cylinder axis). Firstly, the cross-sectional area  $A$  and perimeter  $P$  for the channels on each section were measured. Then, the shape characteristics roundness and equivalent diameter were analysed to evaluate the geometric accuracy of the channels. The roundness  $\Phi$  was calculated as:

$$\Phi = \frac{4\pi \times A}{P^2} \quad (1)$$

wherein a roundness of 1 corresponds to an ideal circular shape.

The equivalent diameter  $D_e$  relates to the projected circular shape of the corresponding cross section and was determined as:

$$D_e = \sqrt{\frac{4 \times A}{\pi}} \quad (2)$$

Mean values of the equivalent diameters and roundness were computed over the length of the channel from the analysed sections. The channel morphology was further characterized by means of the local principal curvatures of the channel surfaces. To this end, the principal radii of curvature  $r_1$  and  $r_2$  of each point on the surface were determined, from which the two principal curvatures,  $\kappa_1=1/r_1$  and  $\kappa_2=1/r_2$ , were computed. First, a surface of the voxel-based volume was created from the segmented surface using the software AVIZO. The resulting surface is formed by connected local triangular approximations. The curvatures were then calculated considering two direct neighbours to a certain triangle of the surface and the initial curvature values were smoothed by averaging them four times with the curvature values of direct neighbour triangles (more details in our previous work [2]). The local mean curvature  $H$  is expressed as:

$$H = \frac{\kappa_1 + \kappa_2}{2} \quad (3)$$

The reconstructed 3D surfaces were compared to a nominal target diameter of 2 mm, resulting in an analysis of geometric variation as a function of radial orientation in the channel.

Importantly, with this analysis data a measure of the three-dimensional roughness was also obtained in form of the local  $S_z$  values according to the EN ISO 25178 standard.

### 3 Channel surface analysis results before and after treatment

Figure 2 (c)) always result in very high roughness  $S_z$ , which is inherent to the LPBF process. As downskin surfaces typically lack sufficient support from the powder bed below, these surfaces locally acumulate more heat, leading to larger and deeper melt pools and the formation of fused conglomerates of round shapes up to 200 μm in size at the overhanging side. In addition, all surfaces show inherent entrapment and adhesion of unmelted powder particles, which also deteriorate the surface quality and significantly affect quality characteristics such as shape roundness and equivalent diameter.

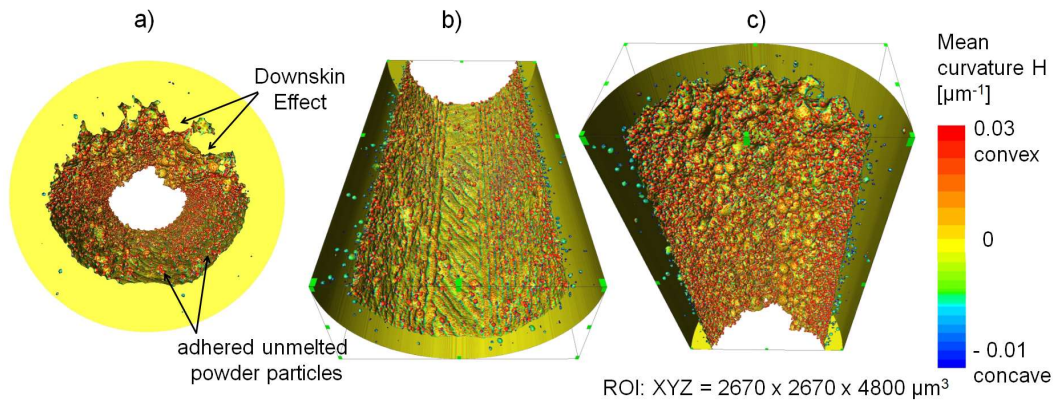


Figure 2: 3D perspective view of the inner surface of a channel produced horizontally at 0° (a), its lower (b) and upper (c) parts. The surface coloring corresponds to the numerical values of the mean curvature H.

A 3D height profile, represented as the deviation from the nominal channel surface (target shape), is shown in Figure 3 for a horizontally 3D-printed channel. Different inward melting effects of the unsupported downskin regions can be detected: besides the formation of surface defects such as adhering, partially melted residual powder particles, the largest contribution is caused by melt beads, leading to a highly deteriorated manufacturing accuracy and, consequently, a significant increase in internal roughness  $S_z$  up to 800  $\mu\text{m}$ .

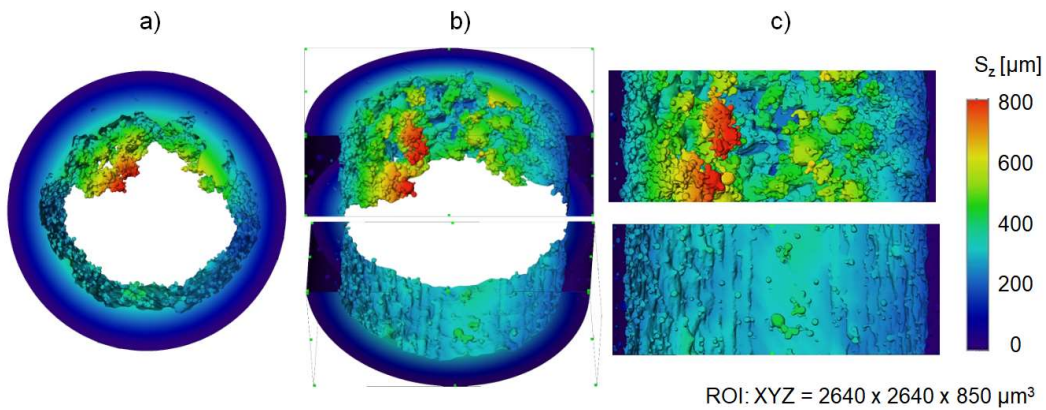


Figure 3: Example of the 3D analysis of the roughness  $S_z$ , calculated as the deviation from the nominal surface of a channel with a target diameter of 2000  $\mu\text{m}$ . A horizontally produced channel (0°) is represented: 3D orthographic view (a), upper and lower halves (b) with their deployed profile (c). The surface coloring corresponds to the roughness  $S_z$ .

The channel quality changes dramatically with the orientation in LPBF: From a flattened and irregular channel shape with a multitude of adhering powder particles and melt beads at 0° (Figure 4(a)), the channels become more uniform with a circular cross section when the orientation approaches 90° (Figure 4 (d)). The roundness of the channel shape  $\Phi$  changes accordingly from  $0.34 \pm 0.08$  to  $0.93 \pm 0.03$ .

The qualitative characteristics of the surface finishing treatment by method 1 are shown in Figure 5 and quantitative characteristics in Figure 6. The roundness  $\Phi$  of the 0° (horizontal) and 30° channels is significantly improved by the treatment from  $0.34 \pm 0.08$  to  $0.78 \pm 0.04$  and from  $0.47 \pm 0.11$  to  $0.80 \pm 0.05$ , respectively. The equivalent diameter  $D_{eq}$  also increases from  $1741 \pm 23$  to  $2055 \pm 8$   $\mu\text{m}$  and from  $1861 \pm 13$  to  $2096 \pm 11$   $\mu\text{m}$  (for 0° and 30°, respectively), slightly exceeding the design diameter of 2000  $\mu\text{m}$ . Clearly the flattening due to degraded downskin surfaces is strongly reduced at build angles  $\geq 60^\circ$ . Inclined 60° and vertical (90°) channels show much smaller further improvements in roundness from  $0.71 \pm 0.12$  to  $0.85 \pm 0.03$  (60°) and from  $0.91 \pm 0.03$  to  $0.92 \pm 0.04$  (90°), with equivalent diameters increasing from  $1886 \pm 13$  to  $2126 \pm 3$   $\mu\text{m}$  and from  $1976 \pm 3$  to  $2162 \pm 3$   $\mu\text{m}$  (for 60° and 90° respectively).

The roundness of channels in vertically oriented (90°) specimen still deviates slightly from its ideal shape ( $\Phi = 1$ ) even after post-treatment with a value obtained at  $0.92 \pm 0.04$ , because unmelted powder particles washed away by the etching liquid jet leave characteristic recesses of up to 20÷40  $\mu\text{m}$  on the inner surface of the channel. This can be observed in Figure 5 (d). The material removal during surface post-treatment also leads to an increase of the average channel diameter compared to the nominal one from  $\sim 30$   $\mu\text{m}$  at 0° orientation to  $\sim 80$   $\mu\text{m}$  at the 90° orientation. This can be taken into account in the design of channel geometries, allowing to precisely meet the target diameter after completing the steps of the manufacturing chain.

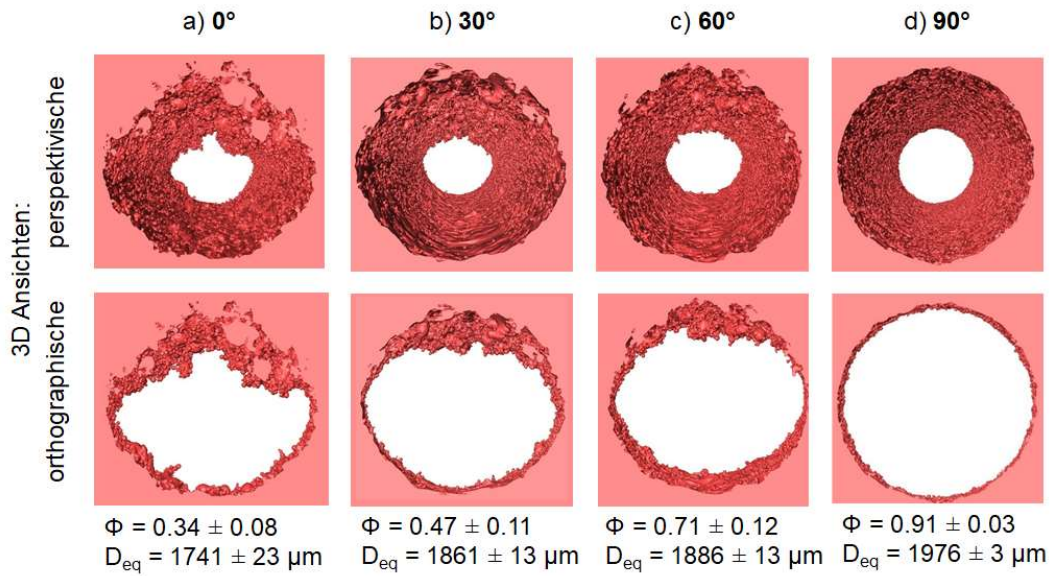


Figure 4: Evolution of the channel profile as function of the build direction of as-built channels: for 0° (a), 30° (b), 60° (c) and 90° (d) inclinations to the working platform. Top row are 3D perspective views, and bottom – orthographic ones. Roundness  $\Phi$  and equivalent diameter  $D_{eq}$  are presented for each channel.

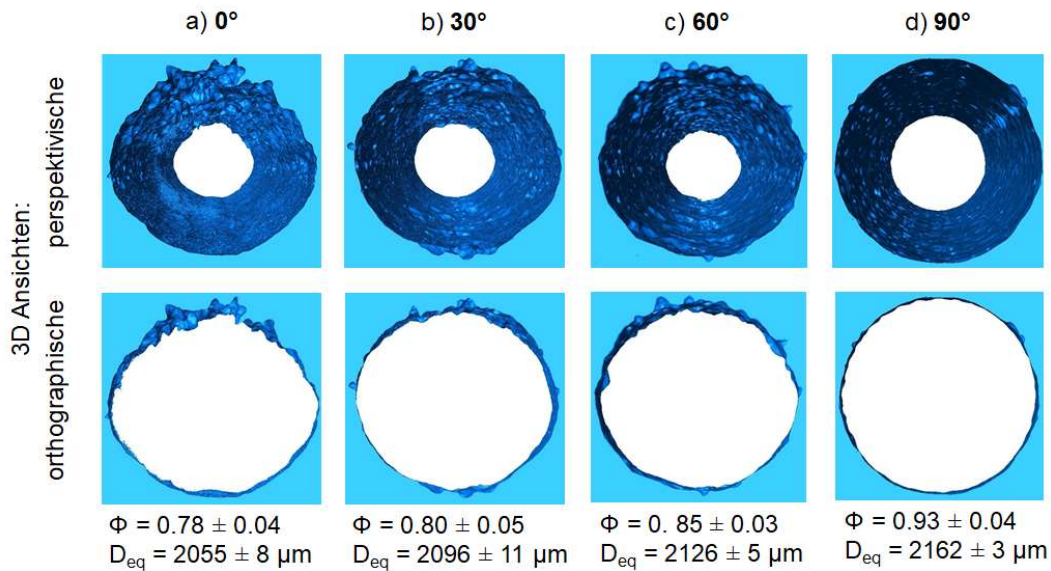


Figure 5: Profile of the channels shown in Figure 4 after etching treatment for the build orientations of: 0° (a), 30° (b), 60° (c) and 90° (d). Top row are 3D perspective views, and bottom – orthographic ones. Roundness  $\Phi$  and equivalent diameter  $D_{eq}$  are presented for each channel. Data obtained for the etching method 1 are presented.

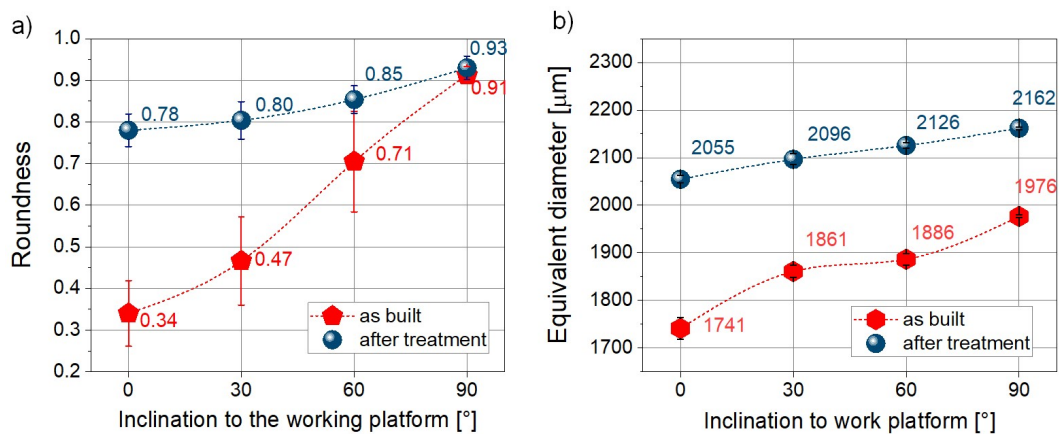


Figure 6: Quantitative analysis of channel treatment efficiency: Roundness  $\Phi$  (a) and equivalent diameter  $D_e$  (b) for different angles of inclination to the working platform. Data obtained for the etching method 1 are presented.

The non-destructive 3D imaging by CT allows analyzing the entire surface of the internal channels, not only single two-dimensional cross sections as in traditional surface measurement methods. For the thin cooling channels used in modern combustion chambers of jet engines, it is important to optimise not only the average quantities, but also the deviation from the average values, visually detectable by possible defects, since the inherent roughness of the LPBF can negatively impact the functionality of cooling systems and result in reduced flow rates due to high friction, possible turbulence, pressure loss and free particles, which can damage other equipment.

As an example, Figure 7 shows a comparative analysis of the different etching techniques: method 1 (Figure 7 (b)) versus method 2 (Figure 7 (c)) for a channel constructed at a 30° inclination (Figure 7 (a)). The visual difference in surface shapes can be evaluated here using an additional quantitative criterion, such as the spatial standard deviation of the  $S_z$  values according to the scale on the right. The deep depressions inherent in method 2 (Figure 7 (c)) result in a high standard deviation in the spatial distribution of roughness:  $\Delta S_z$  increases dramatically from  $\pm 15 \mu\text{m}$  to  $\pm 55 \mu\text{m}$  for downskin areas. Although the average quantitative characteristics of the surface obtained after treatment are approximately the same (same roundness at 0.8 and a small difference in equivalent diameters: 2096 versus 2062  $\mu\text{m}$ ), there is a qualitative difference in morphology: In this particular case, the etching method 2 (Figure 7 (c)) resulted in a less homogeneous surface, as seen when comparing the uniform red top region in Figure 7 (b) and the alternating red-green ridges in Figure 7 (c).

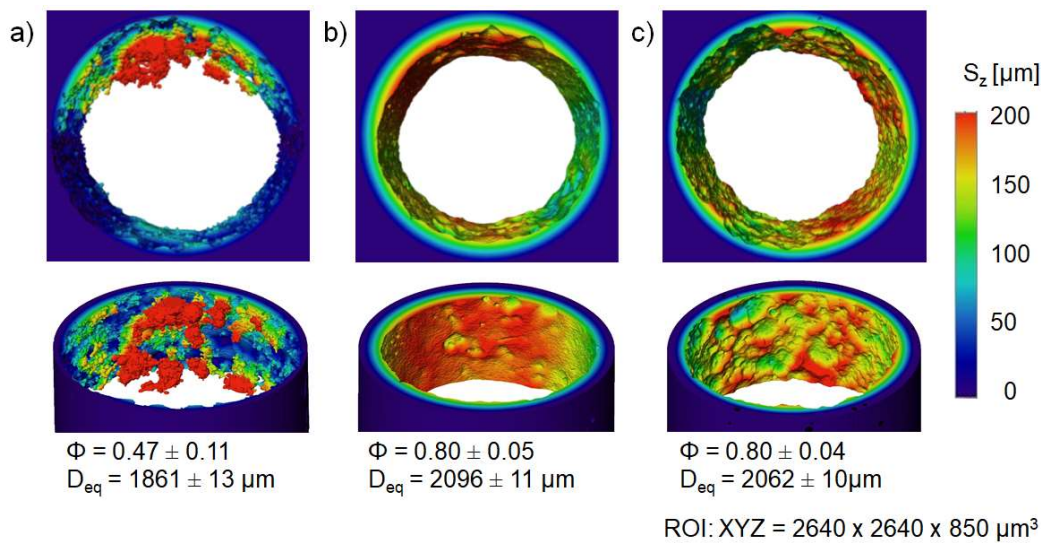


Figure 7: Comparison of the results obtained after different post-treatments: internal channels before post-processing (a) and channels after treatment with method 1 (b) and method 2 (c). The channels in specimen manufactured at a 30° inclination are presented. The color scale on the left is the distance to the nominal surface roughness (radial roughness  $S_z$ ).

In summary, the use of CT characterization of the inner channel surfaces obtained by LPBF in combination with the presented analysis method will allow further optimisation of the quality of inner surfaces, e.g., by means of systematically guiding the optimization of the LPBF parameters, the manufacturing strategies and the post-processing routes. Different etching techniques can be investigated in order to obtain the required surface smoothness and to eliminate the defects inherent to LPBF.

## References

- [1] G. Kasperovich, R. Becker; K. Artzt, P. Barriobero-Vila, G. Requena, J. Haubrich, The effect of build direction and geometric optimization in laser powder bed fusion of Inconel 718 structures with internal channels, *Mat. & Design*, 207 (2021) 109858, <https://doi.org/10.1016/j.matdes.2021.109858>
- [2] G. Kasperovich, J. Haubrich, J. Gussone, G. Requena, Correlation between porosity and processing parameters in TiAl6V4 produced by selective laser melting, *Mat. & Des.* (2016) 105, 160–170, <http://dx.doi.org/10.1016/j.matdes.2016.05.070>